

Sulfur dioxide emissions related to volcanic activity at Asama volcano, Japan

Michiko Ohwada · Kohei Kazahaya · Toshiya Mori ·
Ryunosuke Kazahaya · Jun-ichi Hirabayashi ·
Makoto Miyashita · Shin'ya Onizawa · Takehiko Mori

Received: 13 March 2013 / Accepted: 19 October 2013 / Published online: 14 November 2013
© Springer-Verlag Berlin Heidelberg 2013

Abstract A 40-year-long record of the sulfur dioxide (SO₂) emission rate of Asama volcano, Japan, is presented including high-temporal-resolution data since the 2004 eruption. The 2004 and 2008–2009 eruptive activities were associated with high SO₂ emission, and SO₂ emission rates markedly fluctuated. In contrast, stable and weak SO₂ emissions have been observed for the rest of the investigated interval. The fluctuation of the SO₂ emission rates is correlated with the number of shallow low-frequency B-type earthquakes, implying that increased flows of gas and/or magma induced the B-type earthquakes along the shallow conduit. The total

volumes of outgassed magma during the 2004 and 2008–2009 eruptive activities are estimated to be 1.9×10^8 and 1.5×10^8 m³, respectively. These volumes are about 100–200 times larger than those of the erupted magma, indicating that the large volumes of the magma were outgassed without being erupted (i.e., excess degassing/outgassing). Degassing and outgassing driven by magma convection rather than by permeable gas flow in the conduit is concluded as the probable degassing/outgassing process of Asama volcano based on model examinations, and is thought to occur regardless of the outgassing intensity. Production rates of outgassed magma related to the 2004 and 2008–2009 eruptive periods are estimated to have been 7.4×10^3 and 6.7×10^3 kg/s, respectively. These values are one order of magnitude higher than the average production rate of 0.92×10^3 kg/s for the inactive periods. Increased supply of fresh magma is thought to activate magma convection in the conduit and to thereby increase magma degassing/outgassing.

Editorial responsibility: P. Wallace

M. Ohwada (✉) · K. Kazahaya · R. Kazahaya
Geological Survey of Japan, National Institute of Advanced
Industrial Science and Technology (AIST), Central 7, 1-1-1 Higashi,
Tsukuba, Ibaraki 305-8567, Japan
e-mail: ohwada.m@aist.go.jp

T. Mori
Geochemical Research Center, Graduate School of Science, The
University of Tokyo, 7-3-1 Hongo, Bunkyo-ku, Tokyo 113-0033,
Japan

J. Hirabayashi
Volcanic Fluid Research Center, Tokyo Institute of Technology,
2-12-1 Ookayama, Meguro-ku, Tokyo 152-8551, Japan

M. Miyashita
Seismological and Volcanological Department, Japan
Meteorological Agency, 1-3-4 Otemachi, Chiyoda-ku,
Tokyo 100-8112, Japan

S. Onizawa
Meteorological Research Institute, Japan Meteorological Agency,
1-1 Nagamine, Tsukuba, Ibaraki 305-0052, Japan

T. Mori
Earthquake Research Institute, The University of Tokyo,
1-1-1 Yayoi, Bunkyo-ku, Tokyo 113-0032, Japan

Keywords SO₂ emission rates · B-type earthquakes · Volcanic activity · Degassed and outgassed magma · Convective degassing and outgassing of magma · Asama volcano

Introduction

Volatiles exsolved (“degassed”) from magma are principally released as volcanic gases (outgassed). The compositions and emission rate of volcanic gas provide insights into magma chemistry and volcano dynamics. The monitoring of volcanic gas emissions is particularly useful for forecasting volcanic and outgassing activities. Volcanic gas emission rates are generally obtained from measurements of SO₂ in the plume using ground-based and satellite-based remote sensing techniques (Shinohara 2008; Oppenheimer et al. 2011). The ground-based measurements have been mainly performed

with a correlation spectrometer (COSPEC: Stoiber et al. 1983) and a miniature ultraviolet spectrometer (e.g., mini-DOAS: Galle et al. 2003; FLYSPEC: Horton et al. 2006; COMPUSS: Mori et al. 2007). Sulfur dioxide emission rates at numerous volcanoes obtained by these instruments have been reported and compiled (e.g., Stoiber et al. 1983; Symonds et al. 1994; Andres and Kasgnoc 1998; Shinohara 2008; Oppenheimer et al. 2011, Mori et al. 2013).

Volcanic gas emission is generally characterized by “excess degassing” which means that more gas is exsolved (degassed) and released (outgassed) than could be supplied by volatiles that were dissolved in erupted magma (Andres et al. 1991; Wallace 2001; Shinohara 2008). This “excess degassing” reflects the degassing and outgassing of large amounts of non-erupted magma. The volume of the outgassed non-erupted magma can be estimated by quantifying the SO₂ emission and the dissolved sulfur concentration in the magma. Knowledge of the volume of degassed and outgassed magma makes it possible to evaluate the nature of degassing and outgassing activity and to understand the magma conditions beneath the volcano (e.g., Kazahaya et al. 1994, 2002; Kazahaya and Shinohara 1996; Werner et al. 2011).

Here, we present data and interpretations for temporal variations in the SO₂ emission rates of Asama volcano, Japan, over a 40-year period from 1972. We investigate the relationship between SO₂ emission and seismicity by using high-temporal-resolution monitoring data of SO₂ emission rates after the 2004 eruption. We also discuss the degassing and outgassing processes of Asama volcano based on the calculated volumes of outgassed magma and production rates of outgassed magma estimated from measured SO₂ emissions.

Asama volcano

Asama volcano, located in central Japan, is one of the most active volcanoes in Japan (Fig. 1a). Magmas erupted from Asama volcano are predominantly andesitic in composition. The volcano summit elevation is 2,568 m above sea level, and the active summit crater is 450 m in diameter and 250 m deep. Although the volcano has been relatively quiescent since the 1960s, eruptions have occurred in 1973, 1982, 1983, 2004, 2008, and 2009 (Miyazaki 2003; Nakada et al. 2005; Yoshimoto et al. 2005; Maeno et al. 2010).

Volcanic gases have continuously discharged from the summit crater. Monitoring of SO₂ emission rates at Asama volcano has been performed since the 1970s. In addition, measurement of volcanic gas compositions by Multi-GAS (Shinohara 2005; Shinohara et al. 2011) was started in May 2004 (Shinohara 2013). The Multi-GAS measurements showed no distinctive changes of volcanic gas compositions

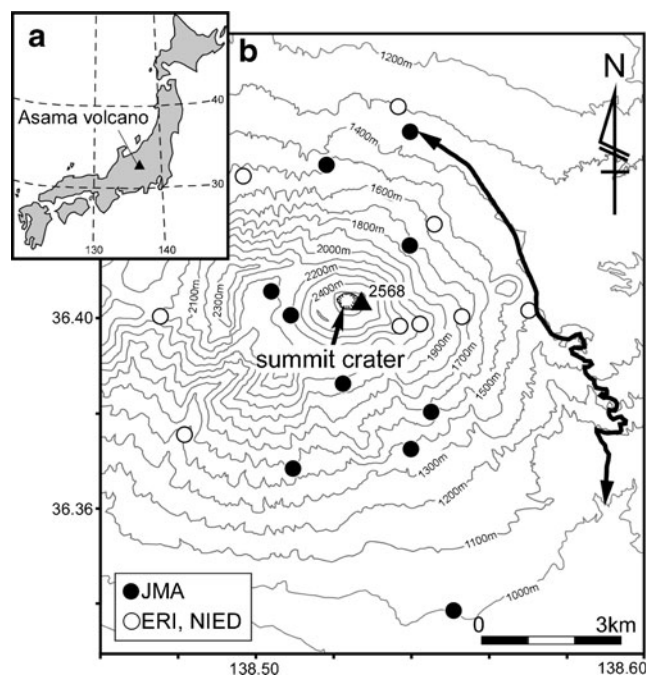


Fig. 1 a Location map of Asama volcano in Japan. b Topographic map for Asama volcano. The contour interval is 100 m; solid line with an arrow shows a typical traverse route for SO₂ emission measurements. Circles are seismic observation stations of each organization. Both newly installed stations after the 2004 eruption and old observation stations are shown

during the period 2004–2012, having constant gas composition with mole ratios of H₂O/SO₂=30, CO₂/SO₂=0.80, HCl/SO₂=0.20 and H₂S/SO₂=0.15 (Shinohara 2013). Asama volcano is subject to detailed monitoring by seismological and geodetic observation networks that have been developed by several organizations. Seismic networks around Asama volcano are operated by the Japan Meteorological Agency (JMA), the Earthquake Research Institute, the University of Tokyo (ERI), and the National Institute for Earth Science and Disaster Prevention (NIED) (Fig. 1b).

The 2004 eruptive activity included the largest magmatic eruptions since 1973 (Nakada et al. 2005), and began with a moderate-sized vulcanian eruption on September 1, 2004. In July 2004, about 2 months before the first eruption, inflation of the volcano was observed by continuous GPS measurements and continued until March 2005 (Aoki et al. 2005, 2013; Takeo et al. 2006). This inflation resulted from magma intrusion as a dike beneath the west flank of Asama volcano to the depth of about 1 km below sea level (b.s.l.) (Takeo et al. 2006; Aoki et al. 2013). Intruded magma then ascended through a conduit extending vertically from about 1 km b.s.l. to near the base of the summit crater (Takeo et al. 2006). A reddish glow had been observed from the end of July 2004, and maximum temperature of the crater had exceeded 500 °C (Japan Meteorological Agency 2005). During September

15–18, frequent strombolian eruptions occurred, and a pancake-shaped lava mound was extruded onto the summit crater floor until October 2004 (Oki et al. 2005). Subsequently, 15 small- and moderate-sized vulcanian eruptions occurred until the end of 2004.

The 2008–2009 eruptive activities started with minor eruptions in August 2008. Inflation of the volcano began in July 2008, a month before the eruption (Aoki et al. 2013). Inflation was caused by a dike intrusion to the depth of 0.7 km b.s.l. (Aoki et al. 2013). It is similar to the 2004 eruptive activity but the position of dike is slightly different. Repeated small/minor eruptions occurred during February 2009, ejecting materials that included only trace amount of juvenile materials; the eruptions mostly recycled near-surface materials (Tanaka et al. 2009; Maeno et al. 2010).

Measurements of sulfur dioxide emission rates at Asama volcano

Measurements of SO₂ emission rates at Asama volcano began in 1972 by a traverse method using the COSPEC (Moffat et al. 1972). Previous studies have reported some of these emission data with regards to volcanic activity at Asama volcano (Okita and Shimozuru 1975; Ohta et al. 1978, 1982; Kyushu University and University of Tokyo 1984, 1986). Measurements after 2003 have also used the COMPUSS, which is a newly built, compact UV spectrometer system in Japan (Mori et al. 2007). Since 2007, all measurements have been carried out by the COMPUSS. We used the improved COMPUSS in which the telescope is directly attached to the spectrometer without an optical fiber connection as with Mori et al. (2006a). Sulfur dioxide emission rates between the COSPEC and COMPUSS measurements have good agreement (Mori et al. 2007). Sulfur dioxide emission rate data from 1972 onwards are summarized in Table 1. Almost all the SO₂ emission rate data from Asama volcano were obtained by the traverse method using a car, with the remainder being obtained by a panning method from an observation site. Sulfur dioxide emission rates measured by the panning method from a distance have been shown to be too low due to the UV dilution effect (Moffat and Millan 1971; Millan 1980; Mori et al. 2006b; Kern et al. 2010). Therefore, our SO₂ emission rates data obtained by panning measurements at Asama volcano may be underestimates. Although these data are given in Table 1, they are not considered further in this paper. Velocities of the volcanic plumes for calculation of SO₂ emission rates were determined from tracings of plume shapes using a theodolite until the 1980s (Ohta et al. 1982, 1988) and by video camera since the 1990s. Measurements of plume velocity using the video camera were performed before and after each SO₂ emission measurement. The plume direction was inferred based on the

position of the maximum measured SO₂ in the plume using traverse measurements. An average value of the plume velocities measured before and after each traverse measurement was used as the velocity value.

Sulfur dioxide emission rates from 1972 are shown in Fig. 2. The SO₂ emission rates during the eruptive and active periods were very high compared with those during the inactive periods. Asama volcano steadily emitted SO₂ gas with an average flux of 2.2 kg/s during all inactive periods (1972, 1975–1980, 1984–2002, 2006–2007, and 2010–). During the recent eruptive activity that started in September 2004, the SO₂ emission rates reached up to 53 kg/s, which is the highest since the observations began at the volcano. The most recent eruptive activity (February 2009) was also characterized by high SO₂ emission rates of 47 kg/s. Since 2000, the SO₂ emission rates have become markedly high as compared with those prior to 2000.

Sulfur dioxide emission rates and B-type earthquakes since 2004

Temporal variations in SO₂ emission rates from July 2004 (i.e., 2 months before the 2004 eruption) are shown in Fig. 3a. Time series of SO₂ emission rates consist of (a) periods of high SO₂ emissions with large fluctuations (active period) and of (b) periods of low SO₂ emissions with very small fluctuations (inactive period). Based on this distinctive pattern of fluctuation, the activities since 2004 can be divided into four periods; two active periods (I and III) and two inactive periods (II and IV) (Fig. 3a).

Active period I began with the eruption in September 2004. Sulfur dioxide emission rates increased with the eruptive activities, and fluctuated from 16 to 53 kg/s. Even after the eruptive activity ceased, a reddish glow was observed in the crater region. The SO₂ emission rates decreased gradually towards the inactive period, which began in August 2006. During the 2-year-long inactive period II, steady SO₂ emissions occurred with small fluctuations between about 1 and 5 kg/s. In August 2008, active period III started with minor eruptions. During active period III, SO₂ emission rates fluctuated from 5 to 47 kg/s. The inactive period IV began in May 2010 and was continuing as of December 2012. During this period, relatively low SO₂ emission rates of 1 to 5 kg/s have been observed. Sulfur dioxide emission rates during the two inactive periods (II and IV) were equal to those of the inactive periods prior to 2004 (1972, 1975–1980 and 1984–2002) (Fig. 2). Stable and low SO₂ emissions of 2.2 kg/s on average have continued during inactive periods since 1972, and the total amount of SO₂ emission during these periods is estimated to have been 2.2 Mt.

At Asama volcano, B-type earthquakes frequently occurred as shown in Fig. 3b. The B-type earthquakes were characterized by a spindle-shaped waveform (Fig. 4), which is

Table 1 Sulfur dioxide emission rate from Asama volcano, Japan

Date		SO ₂ emission rate			Number of measurements times
		Average kg/s	Min kg/s	Max kg/s	
1972 Jun 01	^a	1.6	1.6	1.7	3
1974 Apr 28	^b	8.7	7.7	9.1	4
1977 Sep 17	^c	0.6	0.6	0.7	2
1977 Sep 20	^c	1.5	0.9	2.1	5
1979 Oct 15	^c	0.3 ^d	0.2	0.5	5
1981 Nov 09	^c	6.7	5.7	8.6	9
1981 Nov 10	^c	5.2	3.3	8.7	16
1981 Nov 11	^c	8.6	5.7	17	12
1981 Nov 12	^c	2.7	1.3	4.2	19
1981 Nov 13	^c	8.8	5.2	14	13
1981 Nov 14	^c	4.3	1.8	7.9	16
1982 Jun 18	^e	4.4	3.8	5.4	3
1982 Jun 19	^e	9.4	7.5	11	8
1982 Jun 20	^e	5.9	2.5	8.2	6
1982 Nov 20	^e	8.2	5.1	13	14
1982 Nov 21	^e	9.1	8.3	13	8
1982 Nov 22	^e	7.5	5.2	11	20
1982 Nov 23	^e	7.8	3.2	14	20
1982 Nov 24	^e	5.7	4.1	8.7	15
1982 Nov 25	^e	5.4	3.4	7.6	12
1983 Dec 05	^e	3.1	2.3	4.4	15
1983 Dec 07	^e	2.3	1.5	3.1	10
1983 Dec 08	^e	5.1	3.7	6.3	8
1983 Dec 09	^e	1.9	1.3	3.0	16
1984 Nov 30	^f	0.7	0.4	1.3	10
1984 Dec 01	^f	2.2	1.1	4.6	13
1984 Dec 02	^f	3.1	1.0	6.5	7
1984 Dec 03	^f	3.2	0.9	6.6	8
1984 Dec 04	^f	3.9	2.4	5.6	19
1984 Dec 05	^f	2.0	0.8	3.8	20
1985 Nov 25	^f	2.5	0.9	3.4	12
1985 Nov 26	^f	4.1	1.3	8.1	12
1985 Nov 28	^f	4.1	1.7	7.3	8
1985 Nov 29	^f	3.6	1.6	8.3	20
1995 May 09		1.2 ^d	—	—	—
2001 Mar 09		4.1 ^d	—	—	—
2002 Apr 19		3.6 ^d	—	—	—
2002 Jun 24		2.4 ^d	—	—	—
2002 Jul 03		6.4 ^d	—	—	—
2002 Jul 04		4.6	4.6	4.6	1
2002 Jul 05		9.3	8.1	10	3
2002 Jul 11		23	21	26	3
2002 Aug 27		26	26	26	2
2002 Sep 10		18	16	20	2
2002 Sep 25		9.3	9.3	9.3	1

Table 1 (continued)

Date		SO ₂ emission rate			Number of measurements times
		Average kg/s	Min kg/s	Max kg/s	
2002 Oct 10		3.5	2.3	4.6	3
2002 Oct 18		10	9.3	13	3
2002 Nov 19		10	6.9	14	6
2003 Jan 16		6.9	5.8	9.3	6
2003 Feb 07		28	22	31	6
2003 Feb 19		15	12	22	7
2003 Mar 14		12	9.3	17	8
2003 Mar 28		24	20	30	3
2003 Apr 18		9.3	5.8	13	7
2003 Jul 15		4.6	3.5	4.6	3
2003 Sep 18		5.2	3.5	6.9	4
2003 Oct 20		2.3	2.3	2.3	1
2003 Dec 08		3.5	3.5	3.5	1
2004 May 13		3.5	3.5	3.5	2
2004 Sep 02		16	6.0	26	10
2004 Sep 03		18	10	28	7
2004 Sep 07		31	19	41	4
2004 Sep 08		22	15	33	8
2004 Sep 13		21	18	24	3
2004 Sep 15		38	29	54	6
2004 Sep 16		38	31	49	6
2004 Sep 24		53	39	64	4
2004 Sep 25		22	19	27	4
2004 Sep 28		27	24	32	5
2004 Oct 01		26	18	32	4
2004 Oct 14		19	16	26	4
2004 Oct 22		21	18	28	8
2004 Oct 28		36	33	38	4
2004 Nov 09		34	25	48	5
2004 Nov 25		44	28	64	6
2004 Nov 26		30	24	34	8
2004 Dec 06		39	20	57	10
2004 Dec 07		27	19	37	14
2004 Dec 17		43	33	50	6
2005 Jan 27		30	25	43	10
2005 Jan 31		34	28	44	3
2005 Feb 09		24	18	30	9
2005 Mar 02		31	21	31	10
2005 Mar 10		40	27	55	7
2005 Mar 11		36	33	41	7
2005 Mar 12		46	32	71	8
2005 Mar 29		29	17	41	9
2005 Apr 21		25	17	31	10
2005 Apr 27		9.3	9.3	9.3	1
2005 May 19		18	16	22	3

Table 1 (continued)

Date	SO ₂ emission rate			Number of measurements times
	Average kg/s	Min kg/s	Max kg/s	
2005 Jun 01	13	23	8.1	7
2005 Jun 24	22	13	31	7
2005 Jul 28	16	12	28	10
2005 Jul 29	16	14	23	5
2005 Aug 22	7.5	3.5	10	3
2005 Aug 30	22	19	23	5
2005 Sep 13	17	9.8	23	5
2005 Sep 14	35	23.1	43	5
2005 Sep 30	2.3	2.0	3.5	4
2005 Oct 13	7.9	6.9	8.7	5
2005 Oct 20	15	12	17	4
2005 Nov 04	10	9.6	16	5
2005 Nov 08	8.1	5.8	12	6
2005 Nov 21	4.6	2.3	6.9	6
2005 Nov 25	4.5	2.7	6.7	5
2005 Dec 28	3.1	1.9	4.1	4
2006 Jan 16	16	10	23	6
2006 Jan 26	15	9.3	22	7
2006 Jan 30	24	19	32	5
2006 Feb 10	13	8.1	20	5
2006 Feb 21	5.4	4.1	7.1	11
2006 Feb 22	6.9	4.6	10	6
2006 Mar 07	9.1	6.4	10	8
2006 Mar 22	4.6	2.3	6.9	5
2006 Apr 18	4.7	2.9	7.9	7
2006 Apr 28	4.9	3.0	6.9	6
2006 May 15	3.5	1.2	8.1	6
2006 May 30	4.6	2.3	9.3	9
2006 May 31	8.7	5.4	13	6
2006 Jun 14	5.8	2.3	10	6
2006 Jul 13	5.8	3.5	6.9	3
2006 Aug 29	1.7	1.2	2.3	5
2006 Sep 19	1.2	1.2	2.3	4
2006 Oct 19	0.9	0.7	1.4	5
2006 Oct 26	0.9	0.6	1.2	7
2006 Nov 06	1.0	0.6	1.4	8
2006 Nov 30	2.1	1.5	2.9	4
2006 Dec 20	2.1	1.0	2.8	8
2007 Jan 16	2.0	1.4	3.7	6
2007 Jan 26	1.4	0.8	2.0	6
2007 Feb 13	1.4	1.2	2.0	5
2007 Mar 07	5.0	3.0	8.8	6
2007 Mar 27	1.0	0.8	1.7	5
2007 Mar 28	1.3	0.9	1.9	7
2007 Apr 20	0.9	0.6	1.2	5

Table 1 (continued)

Date	SO ₂ emission rate			Number of measurements times
	Average kg/s	Min kg/s	Max kg/s	
2007 Apr 26	2.1	1.2	2.3	4
2007 May 16	1.4	1.0	2.3	4
2007 Jun 13	0.8	0.7	1.0	4
2007 Jul 24	2.3	2.3	2.3	3
2007 Aug 09	1.0	0.8	1.2	5
2007 Aug 27	2.3	1.2	3.5	3
2007 Sep 13	1.3	0.9	2.3	5
2007 Sep 20	1.2	1.0	1.2	6
2007 Oct 25	1.2	1.2	1.2	4
2007 Nov 08	0.7	0.5	0.9	8
2007 Nov 26	1.5	1.2	2.3	4
2008 Feb 19	2.1	1.2	2.3	6
2008 Apr 23	0.9	0.7	1.2	6
2008 May 07	1.9	1.2	2.3	5
2008 Jul 17	1.0	0.7	1.2	5
2008 Aug 10	14	13	15	2
2008 Aug 11	15	13	16	4
2008 Aug 14	27	20	34	5
2008 Aug 15	22	17	30	3
2008 Aug 18	20	17	21	2
2008 Aug 20	35	31	38	4
2008 Sep 11	13	9.3	15	4
2008 Oct 02	19	14	29	5
2008 Oct 03	17	15	23	6
2008 Oct 16	17	15	19	4
2008 Oct 28	31	30	34	4
2008 Nov 05	31	24	39	6
2008 Nov 14	24	20	30	6
2008 Nov 20	42	26	54	6
2008 Dec 02	23	21	28	6
2008 Dec 12	23	13	30	6
2008 Dec 16	23	17	28	4
2009 Jan 07	23	15	30	6
2009 Jan 08	28	20	36	4
2009 Jan 27	13	6.9	21	5
2009 Feb 03	48	45	50	2
2009 Feb 04	32	23	36	4
2009 Feb 12	46	43	51	4
2009 Feb 16	42	32	42	4
2009 Mar 11	24	16	29	4
2009 Mar 12	21	16	28	5
2009 Mar 19	24	13	43	8
2009 Mar 30	19	17	22	4
2009 Apr 03	22	20	23	5
2009 Apr 08	21	9.3	34	6

Table 1 (continued)

Date	SO ₂ emission rate			Number of measurements times
	Average kg/s	Min kg/s	Max kg/s	
2009 Apr 13	16	12	24	8
2009 Apr 24	8.1	5.8	10	6
2009 May 18	23	10	34	6
2009 May 20	12	9.3	16	5
2009 Jun 02	9.3	4.6	13	4
2009 Jun 12	9.3	8.1	10	3
2009 Jul 16	4.6	3.5	5.8	2
2009 Sep 08	17	16	20	4
2009 Oct 15	4.6	3.5	4.6	3
2009 Oct 19	9.3	6.9	10.4	3
2009 Oct 22	6.9	4.6	8.1	3
2009 Oct 29	9.3	5.8	11.6	4
2009 Nov 06	19	13	23	3
2009 Nov 10	14	6.9	21	6
2009 Nov 27	16	12.7	21	5
2009 Dec 01	6.4	3.5	12	6
2009 Dec 08	20	12.7	24	5
2009 Dec 15	13	10.4	15	5
2010 Jan 08	10	5.8	13	5
2010 Jan 22	6.9	5.8	8.1	2
2010 Mar 18	3.5	2.3	4.6	6
2010 Apr 06	3.5	2.3	5.8	6
2010 Apr 14	4.6	3.5	6.9	5
2010 Apr 19	6.4	4.6	9.3	4
2010 May 06	2.3	1.2	3.5	4
2010 May 18	2.3	1.2	4.6	6
2010 Jun 17	1.6	1.0	2.3	5
2010 Sep 10	2.0	1.2	2.3	3
2010 Sep 22	3.5	2.3	4.6	5
2010 Nov 25	2.7	2.3	3.5	4
2010 Dec 06	2.3	1.2	3.5	6
2011 Jan 05	3.9	2.3	4.6	5
2011 Feb 02	2.3	2.3	3.5	4
2011 Mar 09	1.2	1.2	2.3	5
2011 Mar 25	2.3	2.3	3.5	4
2011 Apr 13	1.2	1.2	1.2	3
2011 May 19	1.2	1.2	2.3	4
2011 Jun 03	4.6	3.5	6.9	4
2011 Jun 24	4.6	2.3	6.9	4
2011 Sep13	2.3	2.3	3.5	2
2011 Oct 14	2.3	2.3	3.5	4
2011 Nov 04	2.3	2.3	3.5	6
2011 Nov 29	2.3	1.2	2.3	3
2011 Dec 12	4.6	3.5	6.9	5
2011 Dec 28	2.3	2.3	2.3	3

Table 1 (continued)

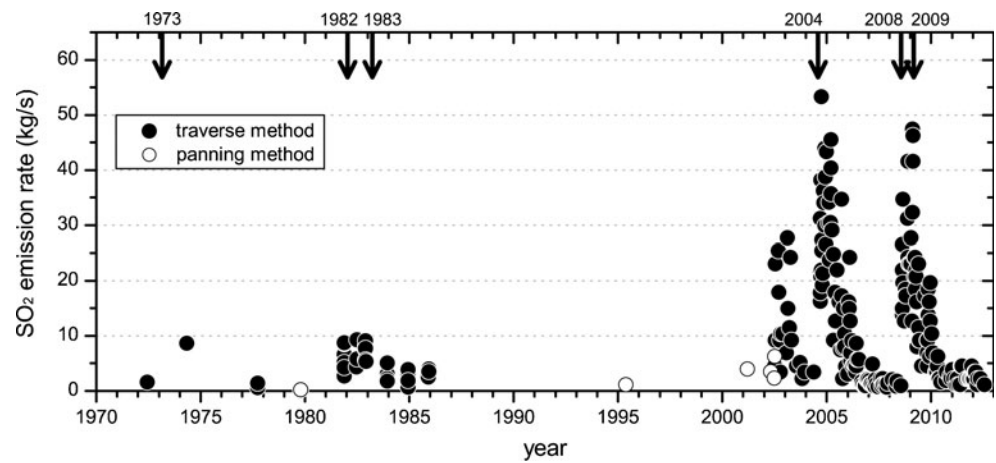
Date	SO ₂ emission rate			Number of measurements times
	Average kg/s	Min kg/s	Max kg/s	
2012 Jan 10	2.3	2.3	2.3	4
2012 Feb 03	3.5	2.3	4.6	2
2012 Feb 13	3.5	2.3	5.8	6
2012 Mar 14	1.2	1.2	2.3	4
2012 Mar 27	2.3	1.2	3.5	5
2012 May 07	2.3	1.2	2.3	6
2012 Jul 17	1.2	0.8	2.3	5
2012 Oct 11	1.2	1.2	2.3	4
2012 Nov 07	2.3	2.3	3.5	4
2012 Dec 05	2.3	2.3	3.5	3

^a Moffat et al. (1972)^b Okita and Shimozuru (1975)^c Ohta et al. (1982)^d Data obtained by panning measurements^e Kyushu University and University of Tokyo (1984)^f Kyushu University and University of Tokyo (1986)

– no data

lacking distinct P phase and S phase signatures (Funasaki et al. 2006). This seismicity has been monitored with short-period seismometers. Most of the B-type earthquakes at Asama volcano are characterized as low-frequency (BL-type) earthquakes (Funasaki et al. 2006) whose dominant frequency is 1–2 Hz (Fig. 4a; Sawada 1994). The rest of the B-type earthquakes are high-frequency (BH-type) earthquakes of dominant frequency of 5–9 Hz (Fig. 4b; Sawada 1994), which account for 2–30 % (about 10 % on average) and 1–40 % (about 15 % on average) in the B-type earthquakes during active and inactive periods, respectively. The number of B-type earthquakes increased in the active periods by a significant increase of the number of BL-type earthquakes and decreased in the inactive periods (Fig. 3b). The time series of the number of B-type earthquakes and the SO₂ emission rates show a good correlation (Fig. 3). The hypocenters of B-type earthquakes were vertically distributed beneath the summit crater during both active and inactive periods, although the number of earthquakes during inactive periods was lower (Takeo et al. 2006; Aoki et al. 2013). At Asama volcano, very-long-period (VLP) seismic pulses have been observed by broad-band seismometers since 2003 (Yamamoto et al. 2005); the hypocenters of the VLP seismic pulse are located at shallow depths of 100–150 m below the crater (Maeda and Takeo 2011). A VLP seismic pulse would be detected as a B-type earthquake on a short period seismometer. The VLP signals are feeble and difficult to detect

Fig. 2 Temporal variations in SO₂ emission rates at Asama volcano from 1972. Allows indicates the eruption events. Sulfur dioxide emission rates between 1972 and 1985 are cited from Moffat et al. (1972), Okita and Shimozuru (1975), Ohta et al. (1978, 1982), Kyushu University and University of Tokyo (1984, 1986)



at large distances (Yamamoto et al. 2005). In this study, as we used the seismic records from short-period seismometers relatively far from the hypocenter (Fig. 1), so VLP seismic events may be included in the number of B-type earthquakes in Fig. 3. Low-frequency earthquakes (0.5–5 Hz), which include B-type earthquakes are thought to be generated by resonance of a fluid-filled resonator excited by a pressure

disturbance; VLP seismic pulses are thought to be generated by transient pressure disturbance caused by mass transport and/or volumetric change (Kumagai 2009). Kazahaya et al. (2011) found a linear relationship between VLP seismic moments and SO₂ emissions at Asama volcano. Magma ascent to shallower levels within Asama volcano has been inferred from the vertical distribution of hypocenters of the B-

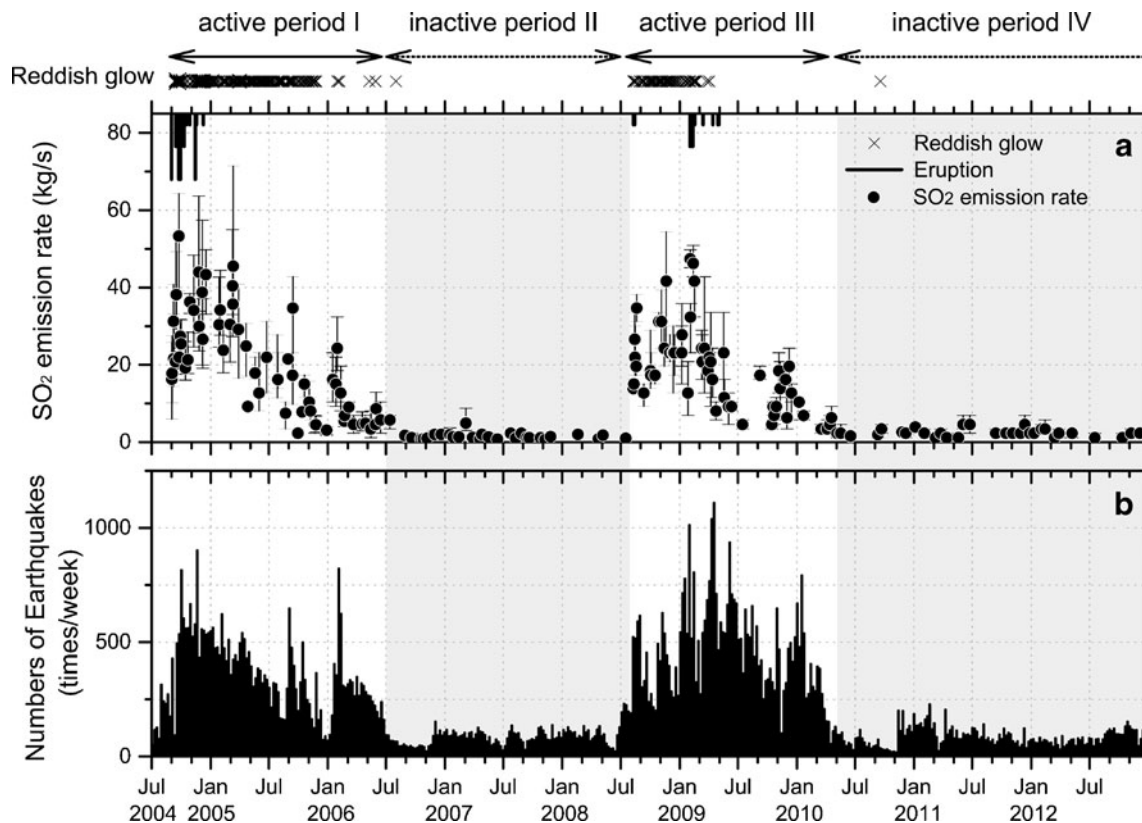
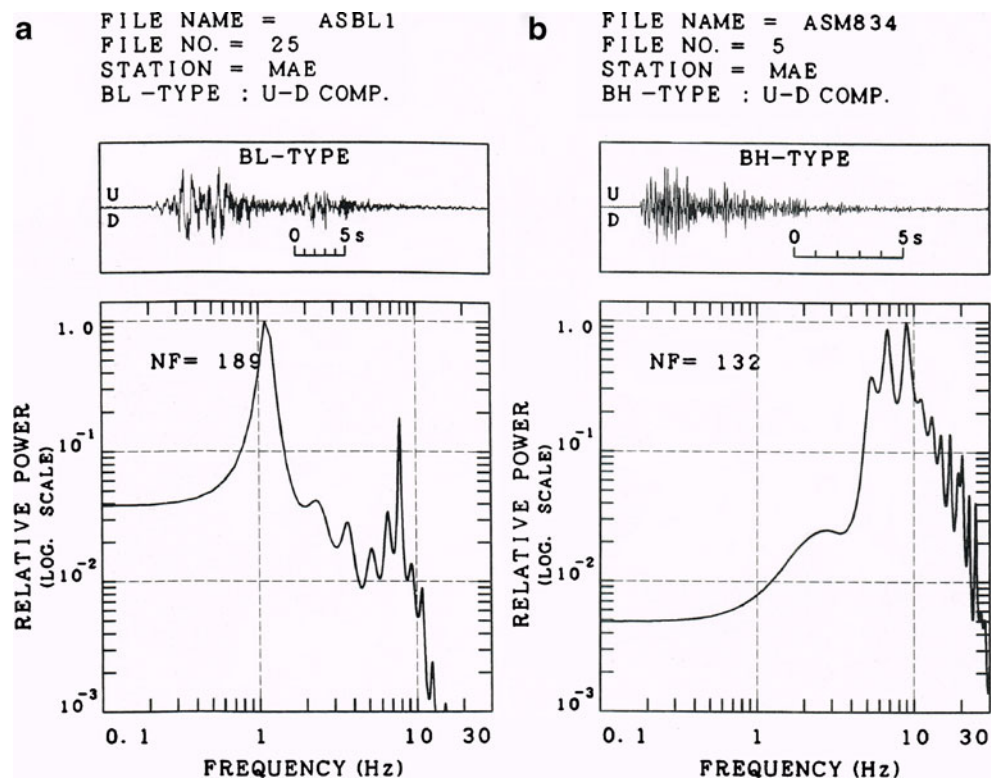


Fig. 3 a SO₂ emission rates from July 2004. The vertical line on the circle indicates the minimum and maximum SO₂ emission rates. The straight lines on the upper part of the graph mark the eruption events,

with the line length representing the scale of each eruption. The cross marks indicate the day when a reddish glow was observed. **b** Temporal variations in the weekly numbers of B-type earthquakes from July 2004

Fig. 4 **a** Velocity spectrum of typical BL-type event from the vertical component (Fig. 7 in Sawada 1994). **b** Velocity spectrum of typical BH-type event from the vertical component (Fig. 6 in Sawada 1994)



type earthquakes and the crustal deformation (Takeo et al. 2006; Aoki et al. 2013). Increased SO_2 emission rates accompanied by increasing numbers of B-type earthquakes in the active periods (Fig. 3) would result from increased flow rate of gas and/or magma in the conduit. B-type earthquakes have been generated throughout the observation period, suggesting that there was movement of the fluid (magma and/or gas) or pressure disturbance relating to SO_2 emission within the volcanic conduit during both active and inactive periods.

Volume estimation of degassed and outgassed magma

The mass of outgassed magma to produce the measured SO_2 emissions (M_{magma}) can be estimated from the SO_2 emission rate (F) and the SO_2 concentration in magma (C_{SO_2}), assuming complete magma degassing and outgassing, as follows:

$$M_{\text{magma}} = \frac{\sum (F \cdot t)}{C_{\text{SO}_2}}, \quad (1)$$

where t is defined as the period of time between two SO_2 emission measurements, and assuming a constant SO_2 emission rate during the period. The scoriae of the 2004 eruption had andesitic compositions ($\text{SiO}_2=61\%$: whole rock composition

analyzed by Miyake et al. 2005) generated by the mixing of the mafic and felsic magmas (Yamaguchi et al. 2005; Ohta et al. 2007). The initial SO_2 concentration of the andesitic magma (C_{SO_2}) is represented by SO_2 concentrations in melt inclusions trapped after magma mixing. Olivine phenocrysts contain sulfur-rich glass inclusions of basaltic ($\text{SiO}_2=49\%$, $\text{SO}_2=4,800$ ppm) to andesitic compositions ($\text{SiO}_2=59\%$, $\text{SO}_2=2,400$ ppm) (Ohta et al. 2007). The SiO_2 content of andesitic glass inclusions are the closest to those of the erupted magma. We thus infer that the SO_2 concentration of 2,400 ppm within this andesitic glass inclusion represents C_{SO_2} before degassing. However, SO_2 may have been exsolved prior to inclusion entrapment, so the C_{SO_2} of 2,400 ppm used here is considered a minimum concentration value; the following estimates for mass and volume of degassed and outgassed magma will thus be maximum values. The masses of outgassed magma (M_{magma}) for the two active periods I and III are estimated to be 470 and 370 Mt, respectively (Table 2). In contrast, the masses of outgassed magma during the two inactive periods II and IV are calculated as 40 and >80 Mt (period IV is continuing as of December 2012), respectively (Table 2). The masses of outgassed magma during the active periods are ca. 5–10 times larger than those in the inactive periods.

The volumes of outgassed magma (V_{magma}) can be estimated using the degassed melt density of $2,500 \text{ kg/m}^3$, which was calculated from the glass compositions of scoria of the 2004 eruption (Table 3; Miyake et al. 2005) and equations in Lange

and Carmichael (1987) and assuming a water-free melt. Estimated volumes of outgassed magma for each active period are $1.9 \times 10^8 \text{ m}^3$ (period I) and $1.5 \times 10^8 \text{ m}^3$ (period III). During the eruption activity of 2004, a lava mound was extruded onto the summit crater floor (Oki et al. 2005). The volume of magma erupted from September to October 2004 was estimated to be ca. $1 \times 10^6 \text{ m}^3$ based on continuous GPS measurements (Murakami 2005) or $2.1 \times 10^6 \text{ m}^3$ ($1.4 \times 10^6 \text{ m}^3$ at the dense rock equivalent volume) based on Airborne Synthetic Aperture Rader measurements (Oki et al. 2005). The volumes of outgassed magma, as estimated from the SO_2 emission rates, are thus ca. 100–200 times larger than the volumes of erupted magma, and represents significant “excess degassing” with emission of gas released from non-erupted magma. Most of the magma that outgassed to emit SO_2 during the active periods was not erupted at the surface, indicating that degassing within the magma chamber and outgassing from it have taken place. The volumes of outgassed magma in the inactive periods were estimated to be $1.6 \times 10^7 \text{ m}^3$ (period II) and $>3.4 \times 10^7 \text{ m}^3$ (period IV). The values are smaller than the volumes of outgassed magma in the active periods, but still larger than those of the erupted magma. Weak and persistent gas emission continued during the inactive periods prior to 2004 (Fig. 2). Total volume of outgassed magma during all inactive periods after 1972 is calculated to be $3.7 \times 10^8 \text{ m}^3$ (Table 2), which corresponds to the SO_2 amount of 2.2 Mt. A large volume of outgassed magma during the inactive periods suggested that the escape of volatiles from the magma chamber has occurred during the inactive periods as with the active periods.

Magma degassing and outgassing processes at Asama volcano

At Asama volcano, there has been intensive outgassing during both active and inactive periods. As previously mentioned, the volume of outgassed magma was: $1.9 \times 10^8 \text{ m}^3$ (period I), $1.6 \times 10^7 \text{ m}^3$ (period II), $1.5 \times 10^8 \text{ m}^3$ (period III), and $>3.4 \times 10^7 \text{ m}^3$ (period IV) (Table 2). Such high volumes of outgassed magma

Table 3 Chemical compositions of glass in the scoria emitted on 23 Sep 2004 at Asama volcano

	SiO ₂	TiO ₂	Al ₂ O ₃	Fe ₂ O ₃	MnO	MgO	CaO	Na ₂ O	K ₂ O
Weight %	73.8	0.9	12.94	3.98	0.05	0.58	2.32	3.08	2.38

Data are from Miyake et al. (2005)

cannot be explained by the volume of erupted magma (about $1 \times 10^6 \text{ m}^3$: Murakami 2005; Oki et al. 2005) or the volume of the dike intruded ($6.82 \times 10^6 \text{ m}^3$ (the 2004 eruption): Aoki et al. 2005; $1.64 \times 10^6 \text{ m}^3$ (the 2008–2009 eruption): Aoki et al. 2013). Understanding the processes by which non-erupted magma outgasses is crucial for investigation of the “excess degassing” problem. Previous studies proposed two “degassing” (outgassing) models to address this problem: the permeable gas flow model (Edmonds et al. 2003) and the magma convection model (e.g., Kazahaya et al. 1994). In this chapter, we will examine these models for outgassing during active and inactive periods at Asama volcano.

Permeable gas flow model

The permeable gas flow model proposed by Edmonds et al. (2003) states that volcanic gases released from a deep magma chamber ascend through a permeable conduit to the surface. A gas emission rate Q_{gas} (in cubic meter per second) is expressed by the following Darcy equation:

$$Q_{\text{gas}} = \frac{\pi \cdot R^2 \cdot k \cdot \Delta P}{\mu_{\text{gas}} \cdot L}, \tag{2}$$

where R is a radius of the conduit (in meter), k is a permeability (in square meter), ΔP is a pressure drop (in pascal), μ_{gas} is a viscosity of volcanic gases (in pascal second), and L is a length scale (in meter). Q_{gas} is given by

Table 2 Average SO_2 emission rate, total mass and volume of outgassed magma and average production rate of outgassed magma at Asama volcano, Japan

	Average SO_2 emission rate	Total mass of outgassed magma	Total volume of outgassed magma ^a	Average production rate of outgassed magma
	kg/s	Mt	m^3	kg/s
Active periods				
Period I (Sep 2004–Jul 2006)	20	470	1.9×10^8	7.4×10^3
Period III (Aug 2008–Apr 2010)	19	370	1.5×10^8	6.7×10^3
Inactive periods				
Period II (Aug 2006–Jul 2008)	1.5	40	1.6×10^7	0.67×10^3
Period IV (May 2010–)	2.5	>80	$>3.4 \times 10^7$	1.0×10^3
All (1972, 1975–1980, 1984–2002, 2006–2008, 2010–) ^b	2.2	>920	$>3.7 \times 10^8$	0.92×10^3

^a The density of degassed melt used $2,500 \text{ kg/m}^3$ (see Table 4)

^b This period includes the inactive periods II and IV

the SO₂ emission rates and the SO₂ molar ratio of 3.7 % (Shinohara 2013); L corresponds to a 1,500-m-long conduit (Aoki et al. 2013). We assume that μ_{gas} is on the order of 10^{-5} Pa s (Edmonds et al. 2003) and ΔP can be taken from inferred by magmatic pressure (i.e., mass of molten magma within the conduit above a given site).

To examine the model, as an input, we used average SO₂ emission rates of 2.2 and 20 kg/s during the inactive and active periods, respectively. Figure 5 shows the model results as a relation between the conduit radius and permeability. The range of permeability is calculated as 10^{-8} to 10^{-12} m². These values are similar to those inferred from Soufrière Hills Volcano (Edmonds et al. 2003). The permeable gas flow model can well explain volcanic gas emission rates at Asama volcano.

Magma convection model

The magma convection model was proposed for degassing at shallower depths (e.g., Kazahaya et al. 1994). A mechanism for magma convection is described as follows: (1) a low-density bubble-bearing magma rises up in a conduit due to buoyancy, (2) the low-density magma releases volcanic gas at the top of the magma-filled conduit, which escapes (outgasses) and thereby increases the density of the magma, and (3) the dense outgassed magma descends in the conduit. This model has been applied to basaltic volcanoes for which magma viscosity is low (Kazahaya et al. 1994, 2004). Here, we examine the likelihood of magma convection at Asama volcano, where the magma is andesitic. As viscosity of andesitic magma is higher than that of basaltic magma, a wider conduit is needed to allow magma convection. An equation describing magma convection was given by Stevenson and Blake (1998) as follows:

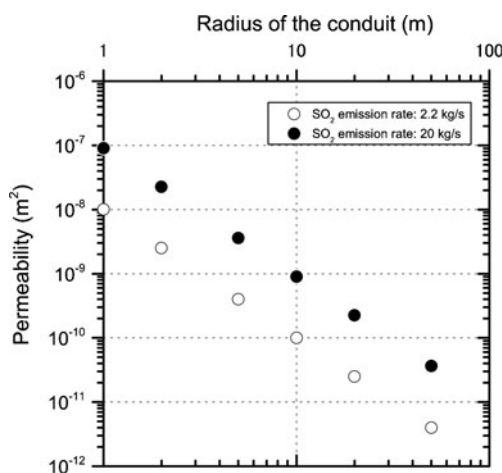


Fig. 5 Relation between radius of conduit and permeability derived from the Darcy's Law. Corresponding SO₂ emission rates are shown in the legends. The fixed values used were $L=1,500$ m, $\Delta P=3.7 \times 10^7$ Pa, and $\mu_{\text{gas}}=10^{-5}$ Pa s. Sulfur dioxide emission rates of 2.2 and 20 kg/s indicate the average values of the inactive and active periods, respectively

Table 4 Description and value of symbols

Symbol	Description	Value	Units
Q_{magma}	Volumetric magma flow rate	–	m ³ /s
R	Radius of conduit	–	m
R'	Radius of upwelling conduit	–	m
R^*	Dimensionless radius of upwelling magma given by R'/R	0.6 ^a	
Ps	Poiseuille number	0.064 ^a	
g	Acceleration due to gravity	9.8	m/s ²
ρ_d	Density of degassed melt	2,500 ^b	kg/m ³
ρ_n	Density of non-degassed melt	2,400 ^b	kg/m ³
$\Delta\rho$	Difference in density to drive convection	100	kg/m ³
μ_d	Viscosity of degassed magma	2.5×10^7 ^c	Pa s
v	Terminal rise velocity of magma	–	m/s

^a Given by Stevenson and Blake (1998)

^b Calculated by Lange and Carmichael (1987) using data from Miyake et al. (2005) and Ohta et al. (2007)

^c Calculated by Giordano et al. (2008) and Tait and Jaupart (1990) using data from Miyake et al. (2005) and Ohta et al. (2007)

$$Q_{\text{magma}} = \pi \cdot (R')^2 \cdot v = \pi \cdot (R^*)^2 \cdot Ps \cdot \frac{g \cdot \Delta\rho \cdot R^4}{\mu_d} \quad (3)$$

Table 4 summarizes the symbols in the equations. The viscosity of magma can be estimated by chemical analyses of glass (for melt viscosity) and the crystal volume fraction of magma (because crystal load affects magma viscosity). Miyake et al. (2005) reported the glass composition (Table 3) and a crystal volume fraction of 0.4 by analyzing a scoria from the 2004 eruption. Water content of melt inclusions is 3.4–4.6 wt% (Ohta et al. 2007). Since water content of the scoria erupted in the 2004 eruption was about 0.1 wt% (Miyake et al. 2005), we infer that almost all water was exsolved from and released (outgassed) by erupted magma. The temperature of the magma chamber was estimated to be 1,323 K (Shimano et al. 2005), and the viscosity of degassed/outgassed magma μ_d was thus calculated to be 2.5×10^7 Pa s (Giordano et al. 2008; Tait and Jaupart 1990). Poiseuille number (Ps) is derived from the ratio of the inferred viscosities between ascending and descending magmas. Assuming a dissolved water content of 3–4 wt% for ascending magma (Ohta et al. 2007), the viscosity of descending magma was about 1100 times greater than that of ascending magma. These values give a Ps of 0.064 (Stevenson and Blake 1998). Dimensionless radius of upwelling magma (R^*) given by the ratio of radii of upwelling magma (R') and conduit (R) is assumed to be 0.6 (Stevenson and Blake 1998). The densities of melts in ascending and descending magmas can be estimated using the method of Lange and Carmichael (1987). We infer that the density differences between ascending and descending magmas can be approximated based on the difference in water

content of the melt phase. In other words, instant outgassing at the top of magma column is assumed, ignoring the effects of crystallization and bubbles in the magma. The melt density difference $\Delta\rho$ was estimated to be 100 kg/m^3 . Given that bubbles in magma significantly decrease the bulk density of the magma in a shallow conduit, this density difference is a minimum estimate. The density difference is proportional to mass rates of magma degassing (Eq. 3), so this minimum estimated difference in density yields the lowest rate of magma degassing and outgassing, and yields the minimum required density difference for magma convection.

Figure 6 shows model results as a function of the conduit radius and the production rates of outgassed magma. Production rates of outgassed magma during the active and inactive periods estimated from the masses of outgassed magma and the duration of each period, were $(6.7\text{--}7.4)\times 10^3$ and $(0.67\text{--}1.0)\times 10^3 \text{ kg/s}$, respectively (Table 2); a conduit radius of 31 m is required to allow magma convection in the active periods. Ground deformation analyses imply that the conduit radius was around 50 m (Aoki et al. 2013). Since the conduit radius required to allow magma convection is less than 50 m, the high volcanic gas emission at Asama volcano can be explained by the magma convection model.

Plausible degassing process at Asama volcano

The high rate of volcanic gas emission at Asama volcano can be explained by either the permeable gas flow model or the magma convection model. To examine plausibility of each model, other kinds of datasets or insights are needed.

For the permeable flow model, magma degasses and outgasses at deeper depths. At Asama volcano, the reddish glows and eruptions were observed as surface phenomena during the active periods. Moreover, the pancake-shaped lava

mound of $2.1\times 10^6 \text{ m}^3$ ($1.4\times 10^6 \text{ m}^3$ at DRE volume) was extruded onto the summit crater floor during the active period (Oki et al. 2005). These facts suggest that volcanic gas emission during the active periods was caused by magma degassing and outgassing of the ascending magma at shallow depths, not at greater depth. Therefore, during active periods at Asama volcano, magma outgassing by permeable flow at depth is unlikely. Magma convection, which allows magma to degas and outgas at shallow depths is more plausible. Even if magma convection into the conduit did occur during active periods, volcanic gas emission during inactive periods by permeable flow from the deeper depth would still be possible. In this case, differences in the composition of volcanic gases during the active (shallow degassing/outgassing) versus inactive (deep degassing/outgassing) periods would be predicted. However, no clear differences in volcanic gas composition between these periods were found (Shinohara 2013). This means that magma needed to ascend to shallower depths during inactive periods as well as during active periods. To explain the constant gas compositions by the permeable gas flow mechanism, the following process would have to occur; a stored magma would need to ascend within the conduit during active periods, and degas and outgas at shallower depths with crystallization of the magma during the inactive periods. However, in this process, the outgassed magma within the conduit generated during the inactive periods must be removed by eruptions in the next active period. As previously mentioned, the volume of outgassed magma was significantly greater than that of erupted magma. Therefore, some other process is required to remove the outgassed magma from the conduit. However, there was no ground deformation or seismic signals such as would accompany removal of the outgassed magma. Consequently, the permeable gas flow model is not credible at Asama volcano.

In the magma convection model, magma degasses and outgasses at shallower depths during both active and inactive periods. Thus the magma convection model can explain the consistent composition of gases. From geophysical observations, Aoki et al. (2013) proposed existence of a magma chamber located west from the summit at 5–10 km b.s.l., a dike located above the magma chamber at 1 km b.s.l., and a winding magma pathway connecting the dike to the 100-m-diameter summit crater. If magma ascends from the magma chamber and goes through the dike, it may not be inferred to be convected within the dike because the thickness of the dike is thought to be no more than several meters. However, at Asama volcano, SO_2 emission persisted even before the dike intrusion in 2004, implying that a magma pathway connecting the deep magma chamber with the shallow part already existed. The magma convection model suggests that the SO_2 emission rates of 2.2 kg/s during inactive periods require a conduit radius of at least 19 m (Fig. 6). The magma pathway radius before the dike intrusion in 2004 is inferred to have been at least 19 m, with presumption that volcanic gas was being emitted as the result of

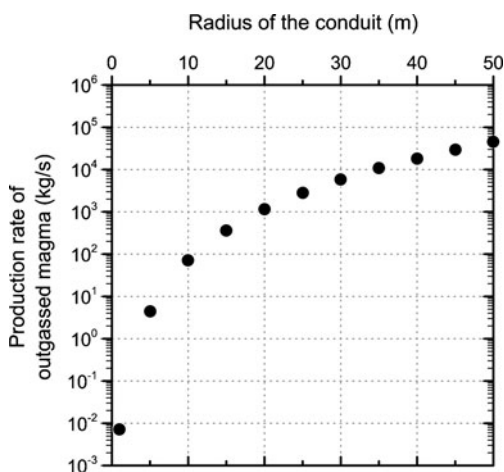


Fig. 6 Model results for magma convection of Asama volcano as a relation between production rate of outgassed magma and radius of conduit. Model parameters used are summarized in Table 4

convective degassing within it. A large amount of magma was supplied from the deep magma chamber to shallow depths by the activity in 2004. The large amount of magma supplied exceeded the capacity of the narrow pathway and caused its destruction, with the excess magma then intruding to form as the dike. Thus, it is possible that magma movement coupled with convective degassing take place along the magma pathway which existed before the dike's intrusion, and prior to emission of volcanic gas during the active periods.

We conclude that magma convection model is more plausible than permeable gas flow as an explanation for the intensive outgassing at Asama volcano. Asama volcano has continued vigorous eruptive activities intermittently. The volcano would need a steady and stiff conduit to support continued outgassing and eruptive activities; the conduit radii in the active and inactive periods are thought to be almost the same. The difference in SO₂ emission rates between these two periods suggests a change in convection intensity. This result from changes in magma properties (viscosity and density) controlled by content of volatiles in melt, crystal and bubble volume fractions and so on. One way to explain the change in convection intensity is that during active periods the magma was more volatile-rich and crystal-poor than during inactive periods, because fresh magma was supplied from a deeper source.

Production rate of outgassed magma by magma convection in the conduit

At Asama volcano, we interpreted continuing SO₂ emissions during the active and inactive periods to be controlled by magma convection. The masses of outgassed magma per unit time resulting from in-conduit magma convection can define as production rates of outgassed magma. Average production rates of outgassed magma during each active and inactive period were calculated 7.4×10^3 kg/s (period I) and 6.7×10^3 kg/s (period III), and 0.67×10^3 kg/s (period II) and 1.0×10^3 kg/s (period IV), respectively (Table 2). The average production rates of outgassed magma during active periods were one order of magnitude higher than those during inactive periods. These differences between the active and inactive periods are inferred to reflect increased magma convection speed in response to supply of fresh (volatile-rich and crystal-free) magma. Moreover, the average production rate of outgassed magma during all inactive periods since 1972 is estimated to be 0.92×10^3 kg/s based on an average SO₂ emission rate of 2.2 kg/s (Table 2). At Asama volcano, during inactive periods, steady SO₂ emission in response to magma convection has continued at this rate. As the supply of fresh magma decreased the melt density and increased ascent velocity of magma in the conduit, accelerated magma convection induces additional B-type earthquakes and high rates of SO₂ emission. In the active periods, simultaneous, pulse-like, and short-period fluctuations of SO₂ emission rate

and seismicity occurred several times (Fig. 3). This fluctuation suggests intermittent magma supply during the active periods. The supply rates of magma would have been transiently higher during the active periods. Moreover, SO₂ emission rates during the active periods I and III were significantly higher than those associated with past active periods prior to the 2004 eruption (Fig. 2), possibly suggesting that the supply rates of magma were much higher in these most recent active periods than previously at this volcano.

In Japan, production rates of degassed (or outgassed) magma have been estimated at several volcanoes. In the Miyakejima's active period in 2000 to 2003, which was characterized by gigantic SO₂ emission, the average production rate of degassed (or outgassed) magma was calculated as 6.7×10^4 kg/s (Kazahaya et al. 2004). At Izu-Oshima volcano, the production rates during two active periods were estimated by Kazahaya et al. (1994): 7×10^3 kg/s (1970–1974) and 1×10^4 kg/s (1988–1990). The production rates of outgassed magma at Asama volcano during active periods were smaller than those at Miyakejima volcano and similar to those at Izu-Oshima volcano. In contrast, at Sakurajima volcano and Satsuma-Iwojima, the production rates of degassed (or outgassed) magma during non-eruptive (inactive) periods have been estimated to be 1.2×10^4 kg/s (1955–1994: Kazahaya and Shinohara 1996) and 2.2×10^4 kg/s (1975–1998: Kazahaya et al. 2002), respectively. The production rate of outgassed magma, 0.92×10^3 kg/s during the inactive periods at Asama volcano, is 1 order of magnitude lower than those at the other volcanoes mentioned here. At Asama volcano, magma convection in the conduit over long periods is suggested to be continually driven by the outgassing at slow rates of magma.

Summary

Asama volcano has alternated between continuous intense SO₂ emission and seismic activity with eruption during active periods, and stable and weak SO₂ emission and low seismic activity during inactive periods. The fluctuations of SO₂ emission rates correlate to the number of B-type earthquakes. Total volumes of outgassed magma for the active periods including to the 2004, 2008–2009 eruptions and the all of the inactive periods since 1972 (31 years) were estimated using SO₂ emission rates and SO₂ concentration in the magma to be 1.9×10^8 , 1.5×10^8 and 3.7×10^8 m³, respectively. Since the volumes of outgassed magma were far greater than those erupted, excess degassing and outgassing have occurred over the whole observational period. By assessing different degassing and outgassing models, we conclude that a magma convection model provides the best explanation for excess outgassing at Asama volcano. Magma convection requires conduit radii of at least 31 and 19 m during active and inactive

periods, respectively. These conduit widths allow magma convection even for the viscous andesitic magma.

The average production rates of outgassed magma during the 2004 and 2008–2009 eruptive activities are estimated to be 7.4×10^3 and 6.7×10^3 kg/s, respectively, values comparable with those for Izu-Oshima volcano after its 1986 eruption. These values are one order of magnitude higher than the rates of 0.92×10^3 kg/s estimated for Asama's entire inactive period. This implies that magma convection was triggered by addition of volatile-rich and crystal-free magma during active periods. The acceleration of magma convection increased the flow rate of gas and/or magma in the conduit, causing the simultaneous increases of SO₂ emission rates and the number of B-type earthquakes during the active periods.

The relation between SO₂ emission and B-type earthquakes presented in this study implies that VLP seismicity at shallow depth is also correlated with SO₂ emission. As the VLP seismic pulses have been observed by broad-band seismometers at the crater rim since 2003, so quantitative comparison between long-term SO₂ emission and VLP seismicity (e.g., seismic moment, number of VLP seismic pulses and so on) is desirable to get new insights into magma degassing processes at shallow depths. The mass of outgassed magma estimated here provides some constraints on mass balance analyses of Asama volcano based on ground deformation studies. Complementary investigations of outflow from the volcano (i.e., the volumes of volcanic gases and volcanic ejecta) and inflation/deflation of the volcano would reveal the details of the magma plumbing system.

Acknowledgments We appreciate Tomoaki Shuto and Hiroaki Kagesawa of the University of Tokyo for their help with fieldwork. The Japan Meteorological Agency kindly allowed us to use their seismic data for Asama volcano. We are also grateful for helpful comments from Dr. Hiroshi Shinohara of the Geological Survey of Japan, AIST. We sincerely thank Associate Editor Dr. Paul J. Wallace, Dr. Marie Edmonds, and Dr. Alessandro Aiuppa for their constructive suggestions and critical comments on this study and for reviewing, and Executive Editor Dr. James. D.L. White for the careful editing of this manuscript.

References

- Andres RJ, Rose WI, Kyle PR, deSilva S, Francis P, Gardeweg M, Roa HM (1991) Excessive sulfur-dioxide emissions from Chilean volcanoes. *J Volcanol Geotherm Res* 46(3–4):323–329. doi:10.1016/0377-0273(91)90091-d
- Andres RJ, Kasgnoc AD (1998) A time-averaged inventory of subaerial volcanic sulfur emissions. *J Geophys Res -Atmos* 103(D19):25251–25261. doi:10.1029/98jd02091
- Aoki Y, Watanabe H, Koyama E, Oikawa J, Morita Y (2005) Ground deformation associated with the 2004–2005 unrest of Asama volcano, Japan. *Bull Volcanol Soc Jpn* 50(6):575–584, in Japanese with English abstract
- Aoki Y, Takeo M, Ohminato T, Nagaoka Y, Nishida K (2013) Magma pathway and its structural controls of Asama volcano, Japan. *Geological Society Special Publications*, 380. doi:10.1144/SP380.6
- Edmonds M, Oppenheimer C, Pyle DM, Herd RA, Thompson G (2003) SO₂ emissions from Soufrière Hills Volcano and their relationship to conduit permeability, hydrothermal interaction and degassing regime. *J Volcanol Geotherm Res* 124(1–2):23–43. doi:10.1016/s0377-0273(03)00041-6
- Funasaki J, Naito H, Kan'no T, Miyashita M, Tikazawa S, Ueda Y, Iijima S (2006) Seismic activity and tilt change observed before the middle scale eruptions of Asama volcano in 2004. *Bull Volcanol Soc Jpn* 51(2):125–133, in Japanese with English abstract
- Galle B, Oppenheimer C, Geyer A, McGonigle AJS, Edmonds M, Horrocks L (2003) A miniaturised ultraviolet spectrometer for remote sensing of SO₂ fluxes: a new tool for volcano surveillance. *J Volcanol Geotherm Res* 119(1–4):241–254. doi:10.1016/s0377-0273(02)00356-6
- Giordano D, Russell JK, Dingwell DB (2008) Viscosity of magmatic liquids: a model. *Earth and Planet Sci Lett* 271(1–4):123–134. doi:10.1016/j.epsl.2008.03.038
- Horton KA, Williams-Jones G, Garbeil H, Elias T, Sutton AJ, Mouginis-Mark P, Porter JN, Clegg S (2006) Real-time measurement of volcanic SO₂ emissions: validation of a new UV correlation spectrometer (FLYSPEC). *Bull Volcanol* 68(4):323–327. doi:10.1007/s00445-005-0014-9
- Japan Meteorological Agency (2005) Abstract of volcanic activities of Asamayama in 2004. Report of Coordinating Comm for Prediction of Volcanic Eruptions 89:11–23, in Japanese
- Kazahaya K, Shinohara H, Saito G (1994) Excessive degassing of Izu-Oshima volcano: magma convection in a conduit. *Bull Volcanol* 56(3):207–216. doi:10.1007/bf00279605
- Kazahaya K, Shinohara H (1996) Excess degassing of active volcanoes: processes and mechanisms. *Mem Geol Soc Jpn* 46:91–104, in Japanese with English abstract
- Kazahaya K, Shinohara H, Saito G (2002) Degassing process of Satsuma-Iwojima volcano, Japan: supply of volatile components from a deep magma chamber. *Earth Planets Space* 54(3):327–335
- Kazahaya K, Shinohara H, Uto K, Odai M, Nakahori Y, Mori H, Iino H, Miyashita M, Hirabayashi J (2004) Gigantic SO₂ emission from Miyakejima volcano, Japan, caused by caldera collapse. *Geology* 32(5):425–428. doi:10.1130/g20399.1
- Kazahaya R, Mori T, Takeo M, Ohminato T, Urabe T, Maeda Y (2011) Relation between single very-long-period pulses and volcanic gas emissions at Mt. Asama, Japan. *Geophys Res Lett* 38:L11307. doi:10.1029/2011gl047555
- Kern C, Kick F, Lübcke P, Vogel L, Wöhrbach M, Platt U (2010) Theoretical description of functionality, applications, and limitations of SO₂ cameras for the remote sensing of volcanic plumes. *Atmos Meas Tech* 3:733–749. doi:10.5194/amt-3-733-2010
- Kumagai H (2009) Volcano seismic signals, source quantification of. In: Meyers RA (ed) *Encyclopedia of complexity and systems science*. Springer, New York, pp 9899–9932
- Kyushu University, University of Tokyo (1984) Variation of emission rates of sulfur dioxide associated with the 1982–1983 eruption at Asama volcano. Rep of Coordinating Comm for Prediction of Volcanic Erupt 30:111–113 in Japanese
- Kyushu University, University of Tokyo (1986) Emission rates of sulfur dioxide from Asama volcano during the period from 1984 to 1985. Rep of Coordinating Comm for Prediction of Volcanic Erupt 37:1–2, in Japanese
- Lange RA, Carmichael ISE (1987) Densities of Na₂O–K₂O–CaO–MgO–FeO–Fe₂O₃–Al₂O₃–TiO₂–SiO₂ liquids—new measurements and derived partial molar properties. *Geochim Cosmochim Acta* 51(11):2931–2946. doi:10.1016/0016-7037(87)90368-1
- Maeda Y, Takeo M (2011) Very-long-period pulses at Asama volcano, central Japan, inferred from dense seismic observations. *Geophys J Int* 185:265–282. doi:10.1111/j.1365-246X.2011.04938.x
- Maeno F, Suzuki Y, Nakada S, Koyama E, Kaneko T, Fujii T, Miyamura J, Onizawa S, Nagai M (2010) Course and ejecta of the eruption of

- Asama volcano on 2 February 2009. *Bull Volcanol Soc Jpn* 55(3): 147–154, in Japanese with English abstract
- Millan MM (1980) Remote sensing of air pollutants. A study of some atmospheric scattering effect. *Atmospheric Environ* 14:1241–1253
- Miyake Y, Takahashi K, Tsugane T, Makino K, Kakuzen H, Nishiki K, Fukui T, Shinshu University Research Group for Asama 04 Eruptions (2005) On the essential ejecta of the September 2004 eruptions of the Asama volcano, central Japan. *Bull Volcanol Soc Jpn* 50(5):333–346, in Japanese with English abstract
- Miyazaki T (2003) Re-examination of the records of activities of Asama volcano. *Bull Earthq Res Inst, University of Tokyo* 78:283–468 in Japanese with English abstract
- Moffat AJ, Millan MM (1971) The applications of optical correlation techniques to the remote sensing of SO₂ plumes using skylight. *Atmospheric Environ* 5:677–690
- Moffat AJ, Nakahara T, Akitomo T, Langal L (1972) Mt. Asama volcano SO₂. Barringer Research Technical Paper 062
- Mori T, Kazahaya K, Oppenheimer C, McGonigle AJS, Tsanev V, Olmos R, Ohwada M, Shuto T (2006a) Sulfur dioxide fluxes from the volcanoes of Hokkaido, Japan. *J Volcanol Geotherm Res* 158(3–4):235–243. doi:10.1016/j.volgeores.2006.04.024
- Mori T, Mori T, Kazahaya K, Ohwada M, Hirabayashi J, Yoshikawa S (2006b) Effect of UV scattering on SO₂ emission rate measurements. *Geophys Res Lett* 33(17), L17315. doi:10.1029/2006gl026285
- Mori T, Hirabayashi J, Kazahaya K, Mori T, Ohwada M, Miyashita M, Iino H, Nakahori Y (2007) A compact ultraviolet spectrometer system (COMPUS) for monitoring volcanic SO₂ emission: validation and preliminary observation. *Bull Volcanol Soc Jpn* 52(2):105–112
- Mori T, Shinohara H, Kazahaya K, Hirabayashi J, Matsushima T, Mori T, Ohwada M, Odai M, Iino H, Miyashita M (2013) Time-averaged SO₂ fluxes of subduction-zone volcanoes: an example of 32 years exhaustive survey for Japanese volcanoes. *J Geophys Res Atmos* 118(5):8662–8674. doi:10.1002/jgrd.50591
- Murakami M (2005) Magma plumbing system of the Asama Volcano inferred from continuous measurements of GPS. *Bull Volcanol Soc Jpn* 50(5):347–361, in Japanese with English abstract
- Nakada S, Yoshimoto M, Koyama E, Urabe T (2005) Comparative study of the 2004 eruption with old eruption at Asama volcano and the activity evaluation. *Bull Volcanol Soc Jpn* 50(5):303–313, in Japanese with English abstract
- Ohta K, Kagiya T, Matsuo N (1978) Remote sensing measurements of sulfur dioxide emissions from the Volcano Asama. *Bull Earthq Res Inst, University of Tokyo* 53(2):533–542, in Japanese
- Ohta K, Kagiya T, Matsuo N, Hirahara S, Hirokawa M (1982) Remote sensing measurements of emission rates of sulfur-dioxide from the Asama Volcano Rep. Joint geophysical and geochemical observations of the Asama volcano in 1981:63–72, in Japanese
- Ohta K, Matsuo N, Shimizu H, Fukui R, Kamada M, Kagiya T (1988) Emission rates of sulfur-dioxide from some volcanoes in Japan. In: Kagoshima International Conference on Volcanoes. Kagoshima, Japan, pp 420–423
- Ohta Y, Miyaghi I, Yamaguchi T, Yamaguchi Y (2007) Search for primary magma: water content of melt inclusions. *Monthly Chikyu* 29(1):16–21, in Japanese
- Oki S, Murakami M, Watanabe N, Urabe B, Miyawaki M (2005) Topographic change of the summit crater of the Asama volcano during 2004 eruption derived from repeated airborne synthetic Aperture radar (SAR) measurements. *Bull Volcanol Soc Jpn* 50(5): 401–410, in Japanese with English abstract
- Okita T, Shimozuru D (1975) Remote sensing measurements of mass flow of sulfur dioxide gas from volcanoes. *Bull Volcanol Soc Jpn* 19(3):151–157, in Japanese with English abstract
- Oppenheimer C, Scaillet B, Martin RS (2011) Sulfur degassing from volcanoes: source conditions, surveillance, plume chemistry and earth system impacts. In: Behrens H, Webster JD (eds) Sulfur in magmas and melts: its importance for natural and technical processes. *Reviews in Mineralogy & Geochemistry, Mineralogical Soc Amer, Chantilly*, pp 363–421
- Sawada M (1994) B-type and explosion earthquakes observed at Asama volcano, central Japan. *J Volcanol Geotherm Res* 63(3–4):111–128. doi:10.1016/0377-0273(94)90069-8
- Shimano T, Iida A, Yoshimoto M, Yasuda A, Nakada S (2005) Petrological characteristics of the 2004 eruptive deposits of Asama volcano, central Japan. *Bull Volcanol Soc Jpn* 50(5):315–332, in Japanese with English abstract
- Shinohara H (2005) A new technique to estimate volcanic gas composition: plume measurements with a portable multi-sensor system. *J Volcanol Geotherm Res* 143(4):319–333. doi:10.1016/j.volgeores.2004.12.004
- Shinohara H (2008) Excess degassing from volcanoes and its role on eruptive and intrusive activity. *Rev Geophys* 46, RG4005. doi:10.1029/2007RG000244
- Shinohara H, Matsushima N, Kazahaya K, Ohwada M (2011) Magma-hydrothermal system interaction inferred from volcanic gas measurements obtained during 2003–2008 at Meakandake volcano, Hokkaido, Japan. In: Inguaggiato S, Shinohara H, and Fischer T (eds) *Geochemistry of volcanic fluids: a special issue in honor of Yuri A. Taran*. *Bull Volcanol* 73(4):409–421. doi:10.1007/s00445-011-0463-2
- Shinohara H (2013) Volatile flux from subduction zone volcanoes: insights from a detailed evaluation of the fluxes from volcanoes in Japan. *J Volcanol Geotherm Res*. doi:10.1016/j.volgeores.2013.10.007
- Stevenson DS, Blake S (1998) Modelling the dynamics and thermodynamics of volcanic degassing. *Bull Volcanol* 60(4):307–317. doi:10.1007/s004450050234
- Stoiber RE, Malinconico LL, Williams SN (1983) Use of the correlation spectrometer at volcanoes. In: Tazieff H, Sabroux JC (eds) *Forecasting volcanic events*. Elsevier, Amsterdam, pp 425–444
- Symonds RB, Rose WI, Bluth GJS, Gerlach TM (1994) Volcanic gas studies: methods, results, and applications. In: Carroll MR, Holloway JR (eds) *Volatiles in Magmas*. *Reviews in Mineralogy, Mineralogical Soc Amer, Washington, D.C.*, pp 1–66
- Tait S, Jaupart C (1990) Physical processes in the evolution of magmas. In: Nicholls J, Russell J (eds) *Modern methods of igneous petrology: understanding magmatic processes*. *Reviews in Mineralogy, Mineralogical Soc Amer, Washington, D.C.*, pp 125–152
- Takeo M, Aoki Y, Ohminato T, Yamamoto M (2006) Magma supply path beneath Mt. Asama volcano, Japan. *Geophys Res Lett* 33(15): L15310. doi:10.1029/2006GL026247
- Tanaka HKM, Uchida T, Tanaka M, Takeo M, Oikawa J, Ohminato T, Aoki Y, Koyama E, Tsuji H (2009) Detecting a mass change inside a volcano by cosmic-ray muon radiography (muography): first results from measurements at Asama volcano, Japan. *Geophys Res Lett* 36: L17302. doi:10.1029/2009gl039448
- Wallace PJ (2001) Volcanic SO₂ emissions and the abundance and distribution of exsolved gas in magma bodies. *J Volcanol Geotherm Res* 108:85–106. doi:10.1016/s0377-0273(00)00279-1
- Werner CA, Doukas MP, Kelly PJ (2011) Gas emissions from failed and actual eruptions from Cook Inlet Volcanoes, Alaska, 1989–2006. In: Moran SC, Newhall CG, Roman DC (eds) *Failed eruptions: late-stage cessation of magma ascent*. *Bull Volcanol*. pp 155–173
- Yamaguchi Y, Shimizu S, Yamaguchi T, Ohta Y (2005) Melt inclusions in phenocrysts and sulfide phases in cinders erupted in the 2004.9.1 eruptive event of Asama volcano. In: *Japan Geoscience Union Meeting 2005, Makuhari, Japan*, V056-015
- Yamamoto M, Takeo M, Ohminato T, Oikawa J, Aoki Y, Ueda H, Nakamura S, Tsuji H, Koyama E, Osada N, Urabe T (2005) A unique earthquake activity preceding the eruption at Asama volcano in 2004. *Bull Volcanol Soc, Jpn* 50(5):393–400, in Japanese with English abstract
- Yoshimoto M, Koyama E, Hirabayashi J, Nakada S (2005) The 2004 eruption of Asama volcano, central Japan. *Bull Volcanol Soc Jpn* 50(5):417–420, in Japanese with English abstract